A MM-WAVE, TABLE-TOP CERENKOV FREE-ELECTRON LASER*

I. de la Fuente#, P.J.M. van der Slot, K.J.Boller
University of Twente, Laser Physics & Non-Linear Optics Group, PO Box 217, 7500 AE Enschede, The Netherlands

Abstract

A Cerenkov Free-Electron Laser (CFEL) has the advantage that the operating frequency increases with decreasing electron beam energy. The low beam energy allows for the construction of compact devices. We have designed and constructed such a device with a footprint of 0.5 m x 1.5 m, an operating frequency of 50 GHz and a design output power of 1 kW CW. We will present the overall design and experimental set-up, and first experimental results.

INTRODUCTION

High frequency microwave radiation has shown to be attractive for several applications such as wireless communication, material processing or microwave chemistry [1]. In some cases, also high output power is required, e.g., mm-wave radar applications that require increasingly higher output powers at higher frequencies [1,2]. However, industrial applications seem to be limited to the operating frequencies of the magnetron, though applications have been studied at higher frequencies.

The CFEL may be a welcome addition to the family of microwave sources as a cost-efficient, compact device capable of delivering kW-level output power at frequencies of up to 100 GHz. Compared to undulator based FELs, they have the advantage of generating higher frequencies at lower electron beam voltages and may be especially interesting for millimetre wavelength generation [3,4].

In order to test this potential of the CFEL and to research (industrial) applications as higher frequencies, a compact CFEL with a footprint of about 0.5 m by 1.5 m (excluding a 19 inch rack for power supplies and control electronics) producing an output power in access of 1 kW CW has been constructed and is currently being commissioned. In the remaining part of this paper we will report on the design and construction of this device and present some preliminary experimental results.

OVERVIEW OF THE SYSTEM

A general overview of the CFEL is presented in fig. 1. The main parts of the system are the electron gun, the interaction area, the outcoupler and the collector. Electrons are accelerated from the electron gun towards the lined cylindrical waveguide that forms the interaction area. The electrons are transported through this section up to the collector by means of an axial magnetic field. An outcoupler separates the generated radiation from the electron beam, while at the same time it acts as the down-stream mirror of the oscillator. Table 1 shows the general design values of the CFEL at the University of Twente.

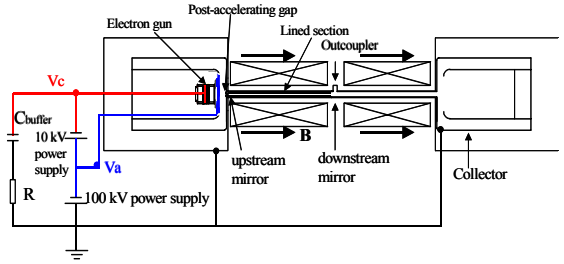

Figure 1. Overview of the CFEL. The depressed collector is initially not installed and instead a buffer capacitor is used to supply the beam current in pulsed operation.

Nominal operational frequency		50 GHz
Electronic tuning range		>10 %
Nominal peak output power		1 kW (10 μs-CW)
Nominal outcoupling		80-9 %
Accelerating voltage		From 65 to 100 kV
Liner	Material	fused GE quartz type 219
	Dielectric constant, ε_r	5.8
	Thickness, d_ε	1.3 mm
	Inner radius, R_d	1.5 mm
	Length, L	250 mm
Magnetic field on axis		0.15 T
Beam diameter		2 mm
Beam current		800 mA
Max HV Power Supply current		30 mA

Table 1: Design values of the tabletop Cerenkov FEL.

Electron gun and beam transport

In the CFEL, the electron beam is generated using a commercially available 10 kV, 800 mA, and gridded thermionic electron gun. The beam is further accelerated to a maximum of 100 kV using a post acceleration section. The grid allows for flexible temporal control of the electron beam and thus also for the generated radiation field. By keeping the acceleration and grid voltage of the (10 kV) electron gun constant, and by varying the post-acceleration voltage, an electron beam is produced with constant current and varying beam voltage.

* Research is funded by the EU, contract **G5RD-CT-2001-00546**
# i.delafuentevalentin@utwente.nl

A combination of commercial air insulated HV power supplies and home build supplies are used for the acceleration, respectively grid, and heater voltages of the electron gun. Short isolating distances are obtained by using SF_6 as an insulating gas and the overall footprint of the complete device could thus be limited to 0.5 by 1.5 m. The design value for the electron beam is 800 mA, whereas the HV power supplies are only able to supply 30 mA. In the final set-up a depressed collector will be installed for cw operation, however, initially the system will be operated in pulsed mode and a buffer capacitor is used to supply the beam current (see fig. 1). Using a buffer capacitor of 70 nF resulted in single pulses of up to 40 μs duration with a rise and fall time of about 0.1 μs, and a train of 10 μs pulses at a few Hz repetition rate. The capacitance, which essentially limits the pulse length, will be increased stepwise to 2 μF, thereby increasing the pulse duration to about one millisecond with a duty cycle of almost 4 %.

First measurements on performance of the electron gun show that the e-beam current varies linearly with the applied grid voltage between 0 and 725 mA and it is independent of the total accelerating voltage. Fig. 2 shows the peak current delivered by the cathode as a function of the grid voltage for a total acceleration of 69.45 kV and a pulse of 10 μs duration.

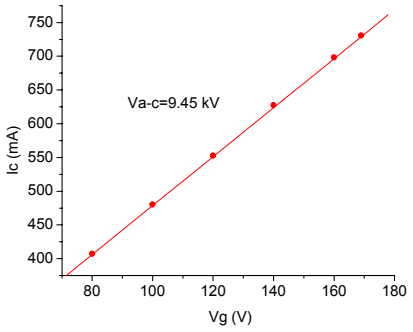

Figure 2: Beam current as a function of grid voltage for a first anode-cathode voltage $V_{a\text{-}c}$ of 9.45 kV.

Characterization of the electron beam transport up to the end of the interaction region, with no liner present, is done by measuring the collected current using a Faraday cup placed just after the first solenoid at the end of the waveguide. The Faraday cup consists of an OFHC copper plate. In addition, the Faraday cup contains a 50 μm-diameter tungsten wire, which can be swept vertically through the electron beam, in front of the plate. The latter gives information about the transverse spatial distribution of the electron beam.
So far, the collected current is 73 % of the current emitted by the cathode and the beam possesses a symmetric distribution in the scan direction. This measured value is consistent with the distance between the Faraday cup and the end of the first solenoid and indicates nearly complete beam transport from gun up to the end of the interaction region. This is concluded from simulations with the software package Trak 6.0 [5], which show that in absence of the second solenoid, Faraday cup collects only a fraction of the electrons within the beam.

Tuning and output characteristics

For sufficiently high frequency the electromagnetic wave propagating through the lined waveguide attains a phase velocity less than the speed of light in vacuum. Such a wave is mainly propagating through the liner and has an evanescent part extending into the vacuum. If the electron velocity is slightly higher than the phase velocity of the wave, the latter produces longitudinal bunches within the electron beam and consequently the beam will coherently amplify the wave, at least as long as it has a longitudinal electric field component. The resonant frequency is defined as the frequency for which the two velocities are equal. As the wave's phase velocity is not only determined by the value of the dielectric constant but also by the geometry, i.e., inner liner radius and waveguide radius, the tuning characteristics can be influenced by appropriate choices of these parameters. It should be pointed out here that variations in, e.g., the inner radius of the liner result in variations of the phase velocity of the wave along the liner and may thus degrade the gain of the device in a way similar to undulator errors in undulator based FELs [6]. This may be especially important for low-gain devices like the current CFEL.
The liner in the actual set-up is a tube made of fused quartz type GE 219 with a specified dielectric constant of 5.8 and dielectric loss less than $\tan\delta = 10^{-4}$. As the exact value of the loss tangent is not known, a value of $1{\cdot}10^{-5}$ is used in the simulations. The liner tube has an inner diameter of 3 mm. At the outside of the tube a thin copper coating is applied, which acts as the waveguide wall, to ensure that no gap exists between the liner and the waveguide.

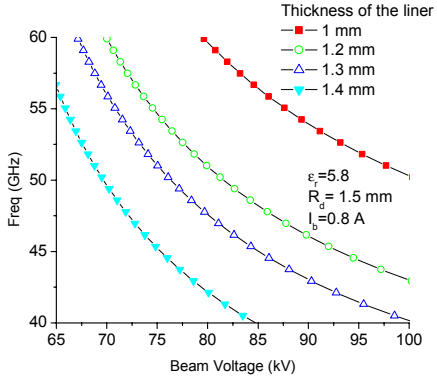

Figure 3: Resonant frequency as a function of electron beam accelerating voltage

Figure 3 shows the calculated output frequency of the CFEL as a function of the total electron accelerating voltage, for several thicknesses of the liner. It can be seen that the expected frequency range covers the interval from 40 GHz to 60 GHz by varying the voltage from 65 to 100 kV, for a 1.2 mm or 1.3 mm thickness of the liner. Larger and smaller values give a more limited tuning range. The thickness of the liner has not only an influence on the tuning characteristics, but it also influences the coupling strength between the electron beam and the co-propagating EM wave. A thickness of 1.3 mm will be chosen for the experiment as with this we expect a higher output power the CFEL (than with 1.2 mm).

The 800 mA current is not enough to provide saturation in a single pass within a reasonable distance, so that the system is configured as an oscillator. To determine the required total reflectivity for a particular length of the liner, fig. 4 shows an example of the calculated output and dissipated power due to dielectric losses as a function of the total reflection coefficient of the oscillator. The reflection coefficient includes all losses except dielectric losses in the liner.

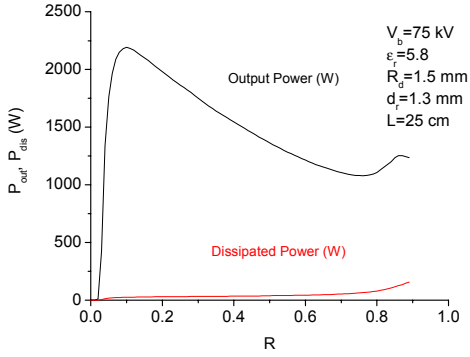

Figure 4: Calculated output and dissipated power due to dielectric losses for different reflection coefficients. The frequency is 50 GHz and a liner length of 25 cm is used.

Fig. 5 summarises the calculated maximum output power from the oscillator, the corresponding dissipated power due to dielectric losses, and the total reflection coefficient necessary to obtain that output power for different values of the liner length. The intra-cavity power should be small to keep the dissipation in the liner and waveguide as low as possible. Therefore, a relative small feedback with a large single pass gain is more desirable than a lower single pass gain and a higher feedback. However, fig. 5 shows that after an initial decrease in dissipated power with increasing interaction length (and thus with increasing single pass gain) it levels off. Apparently, the lower dielectric loss due to a lower intra-cavity power is compensated by the increase in liner length, which results in a higher loss. From fig. 5 it follows that a 20 cm interaction length would be sufficient, leading to a maximum output power of almost 2.3 kW and a required reflection coefficient of about 24 %. The design of the outcoupler indicates that a somewhat lower reflectivity was desirable, to keep mode conversion within the

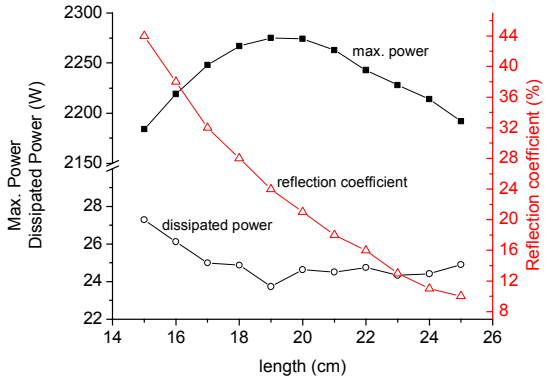

Figure 5: Calculated maximum output power and dissipated power due to dielectric losses with the corresponding reflection coefficient as a function of the length of the liner. The beam voltage is 75 kV and other parameters are as in Table 1.

outcoupler limited. Therefore the construction of the CFEL allows for a maximum liner length of 25 cm.

RF Outcoupler

To form an oscillator, the second anode (at ground potential) is used as the upstream mirror while the RF-outcoupler forms the downstream mirror. The upstream mirror contains a small aperture to pass the electron beam through. The aperture is below cut-off for the frequency range of interest. The RF outcoupler, which is shown in fig. 6, is designed to separate the electron beam from the generated radiation, to reflect part of that radiation and to convert the cylindrical geometry into the standard WR19 waveguide geometry for the output waveguide system. Both the radiation field and the electron beam reach the outcoupler at input port 1. The diameter of the cylindrical input waveguide is tapered down to a smaller value to

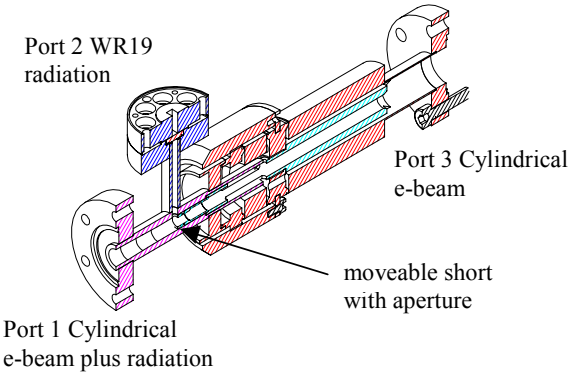

Figure 6: Outcoupler with the corresponding port denomination.

that all other higher order modes above the TM_{01} mode are below cut-off. The radiation is coupled into a standard rectangular WR19 waveguide mounted at a right angle with regard to the input cylindrical waveguide. The amount of coupling, and thus the amount of reflected radiation, can be controlled through the position of a movable short that is connected to port 3. This short contains an aperture that is below cut-off for the resonating frequencies and allows the e-beam to pass straight through to port 3 of the RF-outcoupler. Finally, a 1.85 mm thickness high-density polyethylene vacuum window is placed in the output port 2.

In order to characterize the reflection properties of the RF outcoupler we have measured the S_{11} parameter of port 2 as a function of the position of the short using a Network Analyser with a maximum frequency of 50 GHz. Measurements of the other S-parameters are currently not possible due to the non-standard geometries of port 1 and port 3. The results for a frequency of 50 GHz are shown avoid excessive mode conversion from the TM_{01} mode of the laser into the TE_{11} mode. The final diameter is such in Figure 7 for two cases, one with port 1 open and one when a short is applied to port 1. The measurement data do not change whether port 3 is opened or shorted. This indicates that no measurable radiation is coupled from port 1 or port 2 to port 3. When a short is applied to port 1 the measured S_{11} values indicate that the RF power is dissipated in the RF-outcoupler, which is mainly due to mode conversion. For the positional range of interest (3-6 mm), the dissipated power is less than 7 %, except near the 6 mm position where it increases to 26 %. For port 1 open, the S_{11} ranges from –2 dB to –8 dB when the short is moved from 3 mm to 6 mm, indicating that the desired reflection of 10-20 % is indeed obtained.

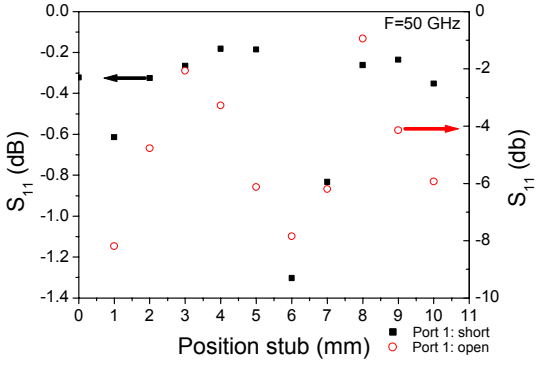

Figure 7: Measured S_{11} parameter at port 2 of the outcoupler for 50 GHz.

FUTURE PLANS

After the electron beam transport is optimised, the RF outcoupler will be installed. Initially, operation and characterization of the laser will be done in pulsed mode, with a progressive increment of the length of the pulses (via increasing the buffer capacitance). The results will provide the necessary data for designing the depressed collector, to be installed subsequently.

Once the source will be fully operational, it will be used to study several novel microwave applications.

REFERENCES

[1] M. Thumm, Free-electron masers vs. gyrotrons: prospects for high-power sources at millimetre and submillimetre wavelengths. *Nuclear Instruments and Methods in Physics Research A* 483 (2002) 186 –194.

[2] S. H. Gold *et. al*., Review of high-power microwave source research, *Rev. Sci. Instrum.* **68,** 11, November (1997).

[3] J.E.Walsh, T.C. Marshall and S.P. Schlesinger, Generation of coherent Cerenkov radiation with an intense relativistic electron beam, *The Physics of Fluids*, **20**, 4, (1977).

[4] E. Garate *et. al*., Cerenkov maser operation at lower-mm wavelengths, *J. Appl. Phys*. **58**, 2, (1985).

[5] Trak 6.0 from *Field Precision*, http://www.fieldp.com.

[6] I. de la Fuente, P.J.M. van der Slot K.-J. Boller, The effect of liner induced phase fluctuations on the gain of a Cerenkov FEL, *in these Proceedings.*